International Research Journal of Engineering and Technology (IRJET) e-ISSN: 2395-0056
Volume: 06 Issue: 10 | Oct 2019 www.irjet.net p-ISSN: 2395-0072

Design, Manufacturing and Testing of Open-circuit Subsonic Wind Tunnels - A Comprehensive Review

Shreyas S. Kharolkar[1], Sarvesh S. Kale[2], Ketan V. Karandikar[3], Pushkaraj D. Sonawane[4]

[1,2]*Final Year B.E. Student, Dept. of Mechanical Engineering, MAEER's MIT Pune, Maharashtra, India*
[3]*Lecturer, Dept. of Mechanical Engineering, MAEER's MIT Polytechnic Pune, Maharashtra, India*
[4]*Assistant Professor, School of Mechanical Engineering, MIT World Peace University, Maharashtra, India*

Abstract - *Wind tunnel is a device that artificially produces airflow relative to a stationary body and measures aerodynamic force and pressure distribution to simulate with actual conditions. Wind Tunnels offer a rapid, economical, and accurate means for aerodynamic research. An important aspect of wind tunnels is their ability to accurately simulate the full complexity of fluid flow. Small-to-medium sized wind tunnels are used in research laboratories for experimental and educational purposes. Though these are relatively smaller in size as compared to commercial wind tunnels, meeting their accurate and precise design and fabrication specifications is quite a tough task. This paper focuses on the design aspects of various wind tunnel components like the test section, contraction cone, diffuser, drive system and the settling chamber. It also discusses various manufacturing approaches considered in previous researches.*

Key Words**: circuit, design, manufacturing, open, review, subsonic, testing, tunnel, wind.**

1. INTRODUCTION

A wind tunnel is used in aerodynamic research to study the effects of air moving past solid objects, the forces acting on them and their interaction with the air flow. It may seem that the use of wind tunnels is obsolete in the age of computers having high computational capability but their application to solve both basic and complex aerodynamic problems is invaluable even today. With their ability to combine various types of data, wind tunnels prove to be a critical device in the efficient and detailed design procedure of anything that involves fluid dynamics. Wind tunnels are used for a varied number of reasons such as testing of prototypes early in their design cycles, or to record a large amount of data while the most important aspect of wind tunnels is that they accurately recreate the full complexity of a fluid flow. While testing new designs and materials, many a times FEA software fail to create the interactions and properties that are not completely known. Here the Wind tunnels step in and help to produce accurate flow modelling results. Also, the usefulness of CFD methods has improved over time but still thousands of hours of wind tunnel tests (WTT) are very much essential for the development of an aircraft, wind turbine, automobile etc. Nowadays there is a growing interest in aerodynamic research from inter-disciplinary fields like automotive industry, architecture, environment, education etc. But with the incapability to obtain accurate solutions with computer software, Low speed wind tunnel (LSWT) have become an integral part of research and design.

The main components of a wind tunnel include an entry section, contraction section, test section, diffuser, and a fan. The entry section also known as the settling chamber helps to makes the air flow laminar and minimize the transverse velocity component. The entry section is followed by the contraction section whose main purpose is to accelerate the flow to a desired velocity in the test section. The test section is that part of the tunnel where the object to be tested is kept along with the measuring instruments and sensors. The Test section is followed by the Diffuser, which helps to steady the flow and maintain constant air speed in the test section. Final section of the wind tunnel is the fan and its housing.

A wind tunnel design mainly depends on its final application. They can be primarily categorized into two basic groups: -

1.1 Open-circuit Design

The open loop wind tunnel s has an intake and an exhaust with no corners and long diffusers. The power required to drive a wind tunnel is high due to the loss of energy in the expelled air to atmosphere. The open circuit wind tunnel is affordable and easy to design. This type of tunnel requires enough free room around it to maintain the quality of air flow. A major advantage of these tunnels is the saving of space and cost along with their immunity to temperature fluctuations. One disadvantage of any open circuit tunnel with an exit diffuser is that the pressure is always less than atmosphere. [1]

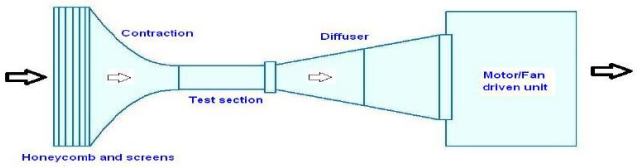

Fig -1: Open loop wind tunnel [1]

The Open circuit wind tunnels are further classified as:

a) Blow down configuration

b) Suck down configuration (as shown in Fig. 1)

These configurations are distinguished by the location of the fan. Blow down tunnels are considered flexible as the fan is at the inlet and the exit diffusers can be skipped to enable access to test samples and instruments. Also test sections can be modified according to the size of the test object. While suck down tunnels are prone to unsteadiness in the return flow. But the swirling effect of air is reduced as the air does not pass through the blower before entering the test section.

1.2 Closed-circuit Design

In a closed-circuit tunnel as shown in Fig. 2, air is recirculated in an enclosed loop and hence requires less power to obtain a given speed. This recirculation of air also increases the overall efficiency of the system. Such tunnels occupy more space and are difficult to design and manufacture. These tunnels can simulate transonic and supersonic air speeds by using an axial fan along with multi-stage compressor. In fact, an open-circuit tunnel is really a closed-circuit tunnel with a poorly designed return leg. [2], [3]

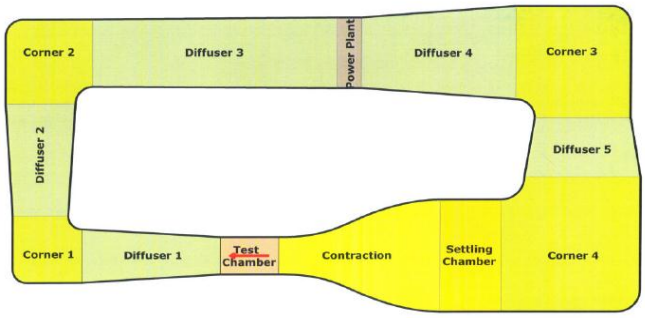

Fig -2: Closed loop wind tunnel [3]

Wind tunnels can also be classified depending on the air flow speed in the test section. Wind tunnels based on speed are:

i. Subsonic; which occur for Mach Numbers less than one, M < 1.

ii. Transonic; which occur for Mach number nearly equal to one, wherein the speed of air approaches the speed of sound; M=1.

iii. Supersonic; which occur for Mach numbers greater than one, 1 < M < 3.

iv. Hypersonic; for speeds greater than five times the speed of sound, M >5.

The design of an aircraft or a vehicle mainly depends on the lift, drag and lift to drag ratio of wings and down force, frontal pressure etc respectively. Hence to study the behaviour of pressure, velocity and forces like drag and lift along with air stream visualization is the basic purpose of a wind tunnel.

2. DESIGN APPROACH

2.1 Settling Chamber and Honeycomb Structure

The entry section, which is also known as the settling chamber, straightens the flow of air, that is the transverse velocity component of incoming air is minimized. From previous studies it has been found that a cell of honeycomb of length 5-10 times the diameter destroys the lateral turbulence of the wind. [4], [5], [6]

The function of the honeycomb is to align the flow with axis of the wind tunnel and break the flow unsteadiness. The function of the screens is to reduce the turbulence levels of the incoming flow along with that the screens break up the large number of turbulent eddies into a number of small-scale eddies that eventually decay. The authors also state that the yaw angle for the incoming air flow should be less than 100 to avoid the stalling of the honeycomb cells. The honeycomb cells can be of different cross-sections such as circular, square and hexagonal. The hexagonal cross-section is the best choice as it has the lowest pressure drop coefficient. The performance of the honeycomb section gives the best performance when the length to diameter ratio is between 7 and 10. Along with that the length of the honeycomb section should be smaller than the smallest lateral wavelength of the velocity variation. [4], [6]

The lowest turbulence in the test section can be achieved by placing multiple screens of different porosities, with the coarsest screen closest to the incoming flow and by placing the finest screen closest to the test section with some free part to decay the fluctuations created by the screen. [7]

To achieve maximum benefit, length of honeycomb section should be taken between 6 to 8 times the cell diameter was mentioned in the paper. The flow velocity profiles can be made uniform using screens that impose a static pressure drop which is proportional to (speed)2 and thus the boundary layer thickness can be reduced increasing the ability to withstand the pressure gradient. [2]

2.2 Contraction Section

The main purpose of the contraction chamber is to accelerate the flow of the air to the desired velocity in the test section. A low entrance velocity is good as it reduces the pressure losses in the wind tunnel. The contraction ratio should be fairly large to eliminate the axial fluctuations in the flow and square cross-section of the contraction section is best. [5]

The contraction ratio (CR) of the contraction section is found to be optimum between the ratios of 7 to 12. [8]

Vortex filaments are stretched in the contraction section which results in the reduction of axial fluctuations, but the lateral turbulent fluctuations are intensified. The length of the contraction section should be sufficiently small as longer

contraction sections cause adverse pressure gradients along the wall, which leads to flow separation. [7]

The separation of flow in the contraction section can be avoided by making it long but the tunnel length also increases along with the cost and exit boundary layer thickness. For smaller wind tunnels, a contraction ratio having value between 6 to 9 is normally used. [2]

2.3 Test Section

The test section is the part where the measurements and observations are made. The dimensions of the test section should be optimum as the velocity through this section goes down as the cross-section of the test section increases. [5]

It is mentioned that the test section should have a constant cross-section area. [9]

The design of the test section should be such that the user can easily access it and can easily install the test models in it. The blockage ratio of 10% is essential corresponding to the frontal area of the test models. The dimensions of the test section should be rectangular with a ratio of about 1.4 to 1. [7]

2.4 Diffuser

The diffuser should have a gently flaring shape which helps to steady the flow and also keep the air speed constant in the test section. The best flow steadiness can be achieved by keeping the diffuser angle at about 50. [5]

The length of the diffuser depends on two variables. The first variable is the diameter or cross-sectional area of the test section and the second variable is the area ratio (AR) of the diffuser section. The standard AR of the diffuser should be around 3 while keeping its equivalent cone angle of 30. [8]

The function of the diffuser is to decelerate the high-speed flow from the test section and to achieve the static pressure recovery. This leads to reduction load on the system. The area of the diffuser should increase gradually along the axis of the wind tunnel to prevent the separation of flow. The divergence half angle of the diffuser walls should be less than 3.50 for conical diffusers. [7]

The optimum diffuser included angle to achieve best flow steadiness is below 50. But for best pressure recovery the diffuser angle should be about 100 and the area ratio should be between 2 to 5. [2]

2.5 Fan Housing and Fan -

The fan power is calculated by the product of the desired volume flow rate and its selection is difficult as we don't know the resistance that the system will offer. The fan and its housing together are the final part of the wind tunnel. [5]

The driving unit for the wind tunnel can be a fan, blower, or even a regulated compressed gas. The designer should also consider the background noise that is made by the fan or the drive system, during the fan selection. [7]

2.6 General Guidelines

There should be a smooth transition between the contraction section and the test section in order to obtain a uniform flow in the test section. In order to achieve this there should be a zero slope at the exit of the contraction section and at the beginning of the test section. First the velocity that the designer expects to be obtained in the test sections needs to be fixed and depending on this velocity, velocity at any cross-section of the wind tunnel can be found out by using the continuity equation. [8]

3. MANUFACTURING APPROACH

The manufacturing of settling chamber with the honeycomb structure is quite difficult. They used Aluminum pipes for the honeycomb as it has low weight and high strength. The structure was assembled using nails and the bond between the pipes was made stronger using adhesive glue. The contraction cone was first designed on SolidWorks and constructed using plywood, nails and adhesive. The top and bottom surface of the test section was fabricated of plywood and side surface was fabricated out of fiber glass. Also, the Diffuser was constructed out of plywood with dampers were used to absorb the vibration. Finally, they selected heavy duty fans having large capacity for high speed air velocity. All these components were properly aligned with the help of dampers, nuts and bolts. Also, the leakage of air was checked at each section of joint. [10]

Firstly, it is necessary to consider what is to be tested in the tunnel in order to decide the size of the test section. Plexiglass was used for the test chamber and a piano hinge was used to attach the plastic viewing window. A major improvement in this wind tunnel was the use of digital measuring scale over mechanical ones. A large supply of 1inch hobby magnets were used to both seal the chamber and prevent air leaks. [11]

Acrylic sheets were used to make the test section visible, which was bolted to the test section frame. An opening was provided on the front side for easy placement of test models. The construction cone, settling chamber and diffuser was constructed by mild steel plate to reduce costs. Readymade screens were purchased from the local market while honeycomb was made in the lab manually using class-A PVC pipe. They mention the importance of fabricating the diffuser as its one end is rectangular while the other being circular. [12]

Flat panels for the construction of all walls of the wind tunnel was suggested. This can be made on site from wood, metal or concrete. It will reduce the transportation costs of

the various parts to the wind tunnel location. They also suggested the use of multi-fan power plant and rectangular ducts to address the low costs of design and construction. [3]

Commercially available honeycomb panels that are used for light weight stiffening of aircraft panels, boat hulls, etc. were selected. The honeycomb was mounted inside a holder constructed from galvanized sheet metal. They used 167 cells across all dimensions. They mention that a square cross section is best for the contraction cone with the contraction ratio being considerably large. Their contraction cone had a straight-sided wedge shape which was fabricated by the contractor. The entry and contraction cone were bolted to each other using flanges with rubber gasket between them. The test section had acrylic plastic viewing port on two sides and a metal flush-fitting access door. The door was clamped to the test section using cam latches, but they suggest the use of piano hinges instead. A hole was drilled on the top to insert the pitot static probe for velocity measurements. Initially their wind tunnel had a diffuser angle of 3.6° but later the diffuser length was increased keeping the angle same. This was done to make space for a larger fan. After a lot of trial and error in the selection of the right fan, a 746W DC motor with variable frequency control powered by a 220 V AC circuit was used. [5]

Two fans which had high efficiency were installed and with that a lot of energy was energy was saved. The motor of the fan was protected using a special hub and the casing and blades of the fan was made of aluminum which reduced its total weight. A controller unit with single inverter was used to properly operate the fans. Considering the cost of metal, wood was chosen for the construction of the diffuser. The diffuser section was made of wood and polycarbonate plates. These are especially light and available in a variety of lengths. The side walls of the test section were made of makrolon type of glass with 98% visibility and 10 mm thickness. One side of the test section had a window which allowed different types of measurements to be taken on the side of the wind tunnel. The contraction cone was built out of wooden planks and beams. Steel angle brackets and screws were used to attach the various beams. While the planks and beams were connected to each other using flat headed screws, bolts and a special type of glue. Three tables were used to support the entire assembly of the wind tunnel. Such a use of disconnected tables reduced the vibration transfer from the drive section to the test section. All corners were sealed with special tape and extra glue which is used for sealing in ventilation systems. This helped to minimize pressure losses and flow irregularities in the wind tunnel. [9]

The test chamber having a square cross section with 45 degrees chamfer was constructed. The diffuser had a length of 332 mm, with an expansion angle of 4°. The honeycomb was 3-D printed and made up of PLA. A commercially available fan was chosen. [13]

4. DETAILED LITERATURE REVIEW

[8] assigned a uniform cross-sectional area (A3) to the octagonal test section of the wind tunnel to reduce the effect of flow eddies, whereas its length was decided according to the design needs. His design was in three phases. In phase 1, length of the diffuser nozzle was calculated. The diffuser nozzle length is dependent on two variables, viz. diameter of the test section and the Area Ratio (AR) of the diffuser nozzle. The typical AR should be kept around 3 with the cone angle of 3°. Since A3 was known, area of the diffuser nozzle exit (A4) was found out by using the following equation

$$AR = \frac{A_4}{A_3} = 3 \qquad (1)$$

Radius of the octagonal test section was found out using the following equation

$$A_3 = 8tan\frac{\pi}{8}R_3^2 \qquad (2)$$

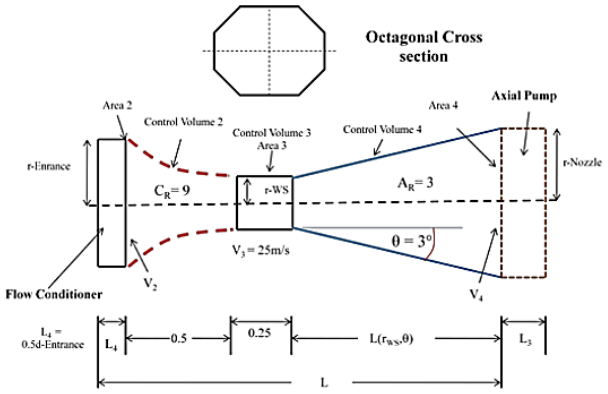

Fig -3: Overall Dimensions of Wind Tunnel [8]

The geometry of the diffuser is as shown in Fig. 4.

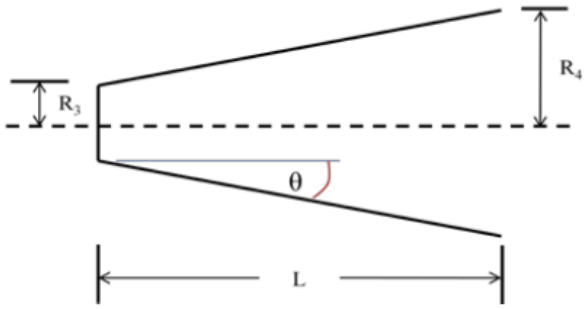

Fig -4: Geometry of Diffuser [8]

Area of the diffuser nozzle at the exit (A4) was determined combining equations (1) and (2). Since A4 was circular, its radius was then calculated by using the following equation

$$R_4 = \sqrt{\frac{A_4}{\pi}} \qquad (3)$$

Finally, length of the diffuser was determined using the following equation and phase 1 was complete.

$$L = \frac{R_4 - R_3}{tan\theta} \qquad (4)$$

An octagonal cross-section was used for the contraction nozzle throughout its length.

A Contraction Ratio (CR) of 9 was used for the design of the contraction nozzle. A2 was calculated using the following equation

$$\boldsymbol{CR = \frac{A_2}{A_3}} \qquad (6)$$

Before proceeding to the next phase, the radius of the contraction nozzle entrance was determined using the following equations

$$A_2 = 8tan\frac{\pi}{8}R_2^2 \qquad (5)$$

$$R_2 = \sqrt{\frac{A_2}{8tan\frac{\pi}{8}}} \qquad (7)$$

In phase 2, the fluid flow was evaluated assuming an incompressible, steady and two-dimensional flow with negligible frictional forces to aid the selection of the pump within the budget. The velocity in the test section was set to 25 m/s. Since the test section shared common inlet and outlet with the contraction nozzle and the diffuser nozzle respectively, the velocities at different section were determined using the Continuity equation as follows

Velocities at the entrance of the contraction nozzle (U2) and that at the exit of the diffuser nozzle (U4) were calculated using the following equations

$$U_2 = \frac{U_3 A_3}{A_2} \qquad (8)$$

$$U_4 = \frac{U_3 A_3}{A_4} \qquad (9)$$

Based on the flow assumptions, Bernoulli's theorem was used to determine the pressures at various sections throughout the tunnel. The ambient velocity (U1) before the contraction nozzle entrance was assumed to be zero and that point was considered as the stagnation point. Pressures were calculated using the following equations

Stagnation Pressure (Pstag)

$$P_{static1} = P_{ambient} = 101.325kPa = P_{stag1} \qquad (10)$$

Pressure at the entrance to the contraction nozzle (Pstatic2), pressure in the test section (Pstatic3), pressure at the diffuser exit (Pstatic4) were calculated using the following equations

$$P_{static2} = P_{stag1} - \rho\frac{U_2^2}{2} \qquad (11)$$

$$P_{static3} = P_{stag1} - \rho\frac{U_3^2}{2} \qquad (12)$$

$$P_{static4} = P_{stag1} - \rho\frac{U_4^2}{2} \qquad (13)$$

Since the pressures at both sides of the pump were known, the pressure recovery provided by the pump was calculated. The fluid pump having the following specifications was selected based on the Volume Flow Rate (VFR) and diameter of the diffuser nozzle

VFR = 683.345 Cubic feet per minutes
ΔP_r = 0.16703 Column inches of water
Diameter = 8.52 in

Design phase 3 was sub-divided into two phases (3-1), (3-2) and (3-3). In phase 3-1, the contraction nozzle contour was designed. The main criterion for the design of the contraction contour was that the velocity of the fluid flow at the exit of the contraction nozzle should be uniform. A smooth transition of the contraction contour from the entrance of the contraction nozzle to the entrance of the test section was obtained. The slope at the entrance of the contraction nozzle was required to be zero. The contraction contour was formed by connecting two cubic arcs at the inflection point as shown in Fig. 5.

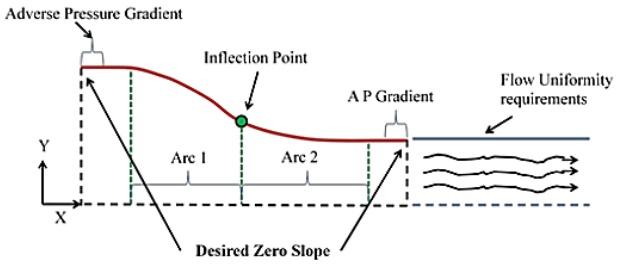

Fig -5: Contraction Nozzle Contour [8]

In phase 3-2, pressure losses at different sections which were needed to be balanced by the fluid pump were calculated by using the following equations

$$h_l = K\frac{V^2}{2g} = \frac{\Delta P}{\rho g} \qquad (18)$$

$$\Delta P = K\frac{V^2}{2}\rho \qquad (19)$$

where K is the loss coefficient, V is the average fluid velocity, and ρ is the fluid density. In general, the loss coefficient K is a function of friction factor and the geometry of the section.

The axial fan requirements are as shown in Fig. 6.

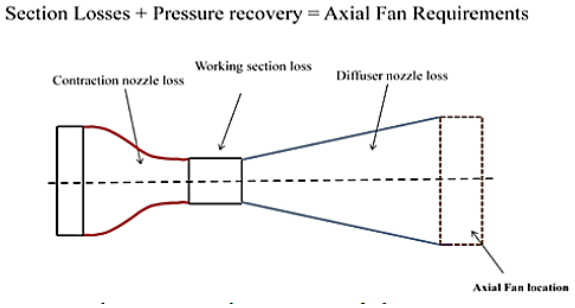

Fig -6: Axial Fan Requirements [8]

The loss coefficient of the working section was calculated as follows

$$K_{ws} = f_{ws}\frac{L_{ws}}{D_{ws}} \qquad (20)$$

w here fws, Lws and Dws are the friction factor, the length and the hydraulic diameter of the working section, respectively. The friction factor may be calculated using the Colebrook equation [4] as:

$$\frac{1}{\sqrt{f}} = -2log_{10}\left(\frac{\varepsilon/D}{3.7} + \frac{2.51}{Re\sqrt{f}}\right) \qquad (21)$$

Assuming zero roughness (ε=0) in the interior of the working section, the Colebrook equation was simplified as follows

$$\frac{1}{\sqrt{f}} = 2log_{10}\left(Re\sqrt{f}\right) - 0.8 \qquad (22)$$

where Re is Reynolds number

$$Re = \frac{\rho V_{avg} D}{\mu} \qquad (23)$$

where ρ and μ are the density and viscosity of the flow, respectively. $Vavg$ is the fluid average velocity in the working section, which was set at 25 m/s by design.

Since the geometry of the test section was known, the hydraulic diameter was calculated using the following equation

$$D = \frac{4A_C}{Per} \qquad (24)$$

where AC is the cross-sectional area, and Per is the wetted perimeter

After this step, the Re was calculated by using equations 22 and 23. Subsequently, the friction factor was calculated and finally the pressure loss in the working section was calculated using equation 19. Based on the total pressure loss, the pressure recovery required by the fluid pump was calculated and a cost-effective pump having the following specifications was selected.

VFR = 683.345 Cubic feet per minutes
ΔP = 0.38828 Column inches of water
Diameter = 8.52 in

Finally, in phase 3-3, the flow was evaluated using CFD simulation.

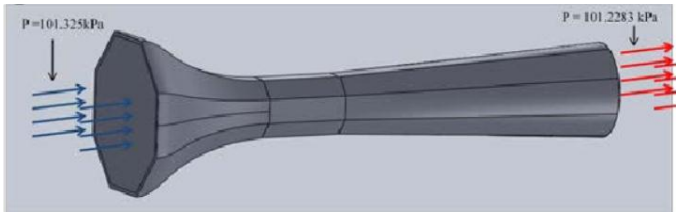

Fig -7: Solid Model of Wind Tunnel [8]

This model was analyzed for any cross-flow using a FEA simulation software. Fig. 8 shows the cross-flow and up-flow.

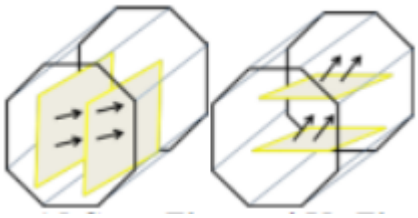

Fig -8: Cross-flow and Up-flow [8]

Both, the cross-flow and up-flow were obtained in negligible amounts which was a good sign. Prior to inserting a model in the test section, the blockage ratio (which should be less than 7.5 %) was calculated by using the following equation

$$BR = \frac{100}{A_{working\ section}}[A_{model}(model\ scale)^2]$$

A model of a sphere was placed in the test section with a blockage ratio of 6.6 % and the velocities around it were studied. According to the simulation, high velocity regions constituted the top and bottom of the sphere while low velocity region was on the left-hand side of it. This conformed well with the theory. The velocity around the sphere is as shown in Fig. 9.

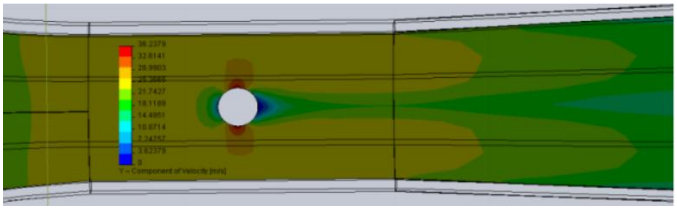

Fig -9: Simulation of Air-flow around a Sphere [8]

Similarly, a NACA 2412 airfoil was analyzed using simulation software with a blockage ratio of 1.2 %. The angles of attack were varied between 0° and 12°. Low-pressure areas were formed on the top of the airfoil while high-pressure areas were formed on its bottom as shown in Fig. 10.

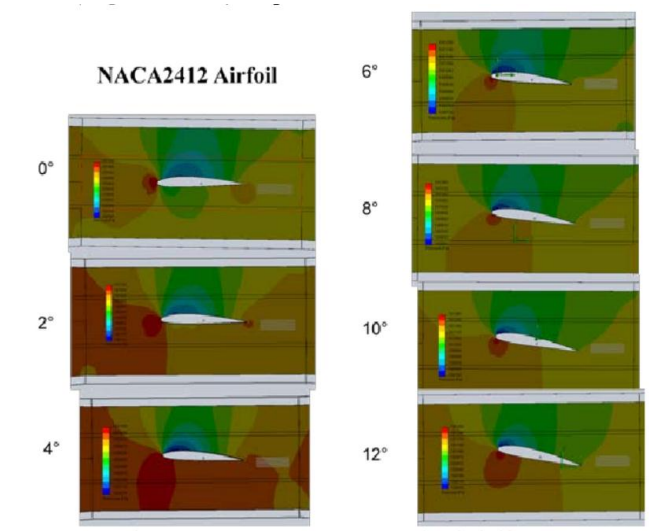

Fig -10: Simulation of Pressure around NACA 2412 Airfoil [8]

These results obtained were compared with the theoretical ones obtained from MATLAB software and gave a good agreement with them.

[14] initially selected the suitable co-ordinates of standard NACA 63-215 airfoil to best fit their test section dimensions as follows

Length = 20 cm

Width = 30 cm

Followed by this, they created a model of the airfoil using 3-D modelling software using these co-ordinates as shown in Fig. 11.

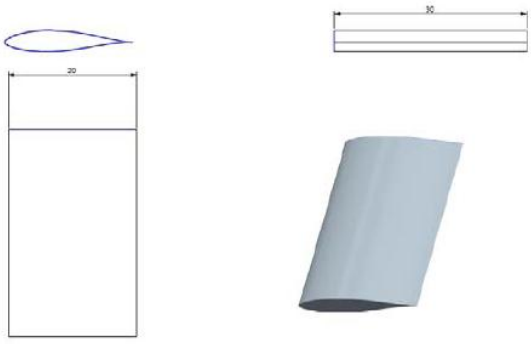

Fig -11: 3-D Model of NACA 63-215 Airfoil [14]

A test section was designed by taking reference of the dimensions of the airfoil as follows

Cross-section of the test section = 30 cm X 30 cm

Length = diameter (d) X 1.5 = 45cm

They chose the length as 50 cm (which is greater than 45 cm)

Its CAD model is as shown in Fig. 12.

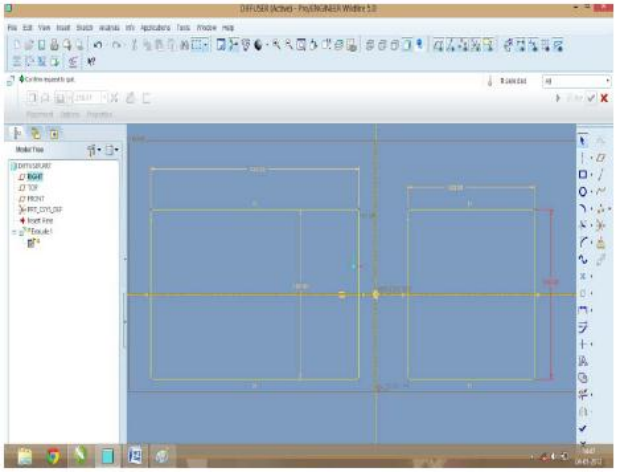

Fig -12: CAD Model of Test Section [14]

The contraction cone was designed by choosing the contraction ratio as 4, as follows

Contraction ratio = (60 X 60) / (30 X 30) = 4

Cross-section = 60 X 60 cm (for outer end) and 30 X 30 cm (for inner end)

Length of the contraction cone = 1.5 X D = 1.5 X 60 = 90 cm

The CAD model of the contraction cone is as shown in the Fig. 13.

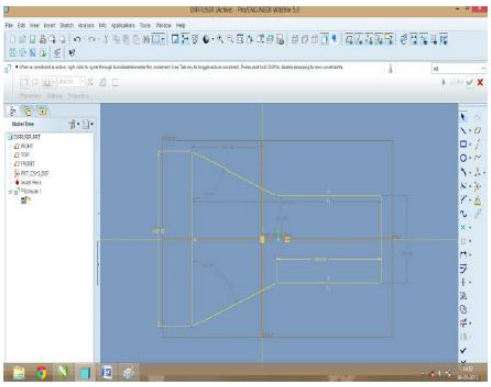

Fig -13: CAD Model of Contraction Cone [14]

The honeycomb was designed following the dimensions of the contraction cone as follows

Cross section = 60 X 60 cm

Length = 10 cm (to minimize the turbulence)

The CAD model of the honeycomb is as shown in Fig. 14.

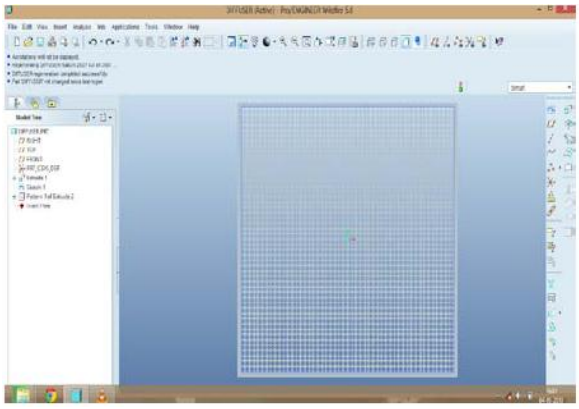

Fig -14: CAD Model of Honeycomb [14]

The settling chamber was designed following the dimensions of the honeycomb structure and hence its dimensions were similar to it. Its CAD model is as shown in Fig. 15.

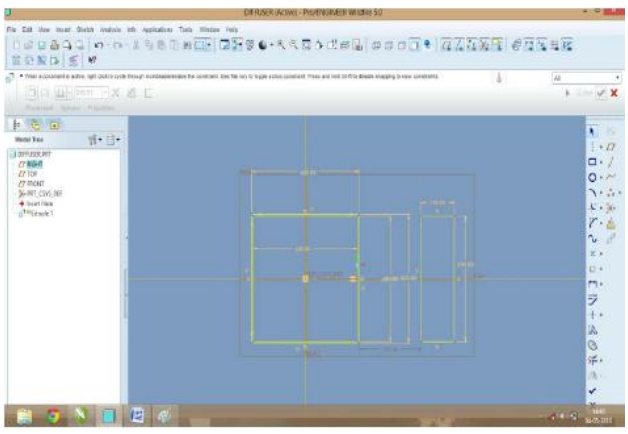

Fig -15: CAD Model of Honeycomb [14]

The diffuser was designed considering the diffuser angle of the diffuser cone. It was designed such that the angle of diffusion (φ) around 5°. Its calculations are as follows

Half angle of diffusion = φ/2 = 2.54

Thus, the outer diameter (Do) of the diffuser was calculated as follows

$$Do = Di + \{2 X (Ld X \tan \varphi/2)\}$$

Where,

Di = inner diameter of the diffuser = diameter of the test section = 30 cm

Ld – length of the diffuser = 90 cm

Hence, Do = 30 + {2 X 90 X tan 2.54}

Do = 30 + 7.984 = 38 cm (approx.)

The CAD model of the diffuser is as shown in the Fig. 16.

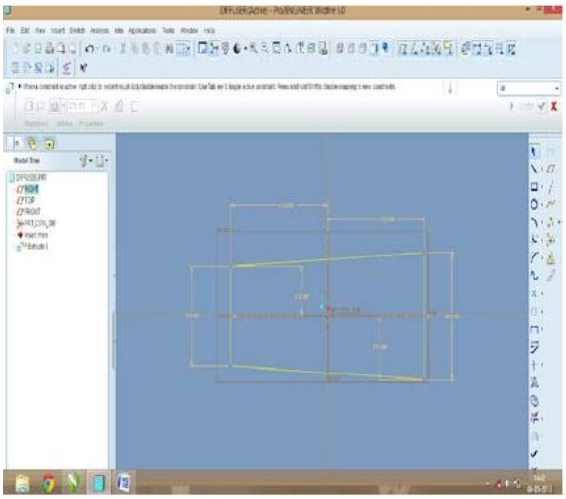

Fig -16: CAD Model of Diffuser [14]

Since the diffuser was located at the extreme end, hence an exhaust fan of ½ HP giving a velocity of 10 m/s was selected instead of an axial fan.

This completed the design procedure of their wind tunnel and the final dimensions were obtained as shown below

Overall length – 10ft
Test Section Length – 50 cm
Test Section Diameter – 30cm
Settling Chamber Diameter – 60cm
Contraction Ratio – 4
Honeycomb Thickness/Cell Size/Cell Count – 10cm
Max Mean Air Velocity – 5.7 m/s
Max Mean output- 4.024 m/s
Diffuser angle- 2.54°

Considering these dimensions, the wind tunnel was fabricated in stages. In stage 1, the contraction cone and diffuser were fabricated using 28-gauge sheet metal since it was easier to bend than the recommended 14-gauge sheet metal. They also verified some designs made up of paper prior to the actual fabrication. The fabricated contraction cone is as shown in Fig. 17.

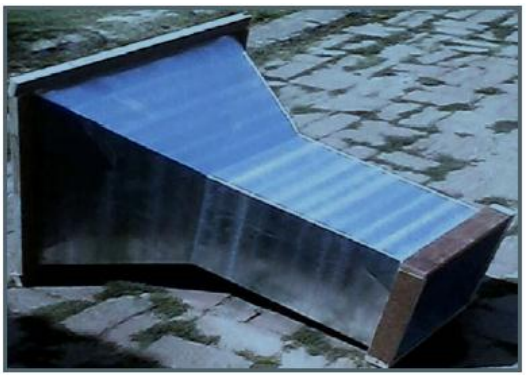

Fig -17: Fabricated Contraction Cone [14]

During the fabrication of the contraction cone, a problem was faced in using welding as the joining process of the two sections since it cannot be used for GI sheet metal. Hence, they chose to pin the sections at the edges at a sheet metal shop. A frame made up of wood ply having a thickness of 2 cm was nailed at the two ends of the contraction cone.

In the next stage, the honeycomb structure was manufactured by using 9260 straws having a diameter of 3 mm and a length of 9 cm. These straws were affixed inside a wooden frame. Finally, considering three sections, the total number of straw pieces was 27800. The cross-section view of the straws is as shown in Fig. 18.

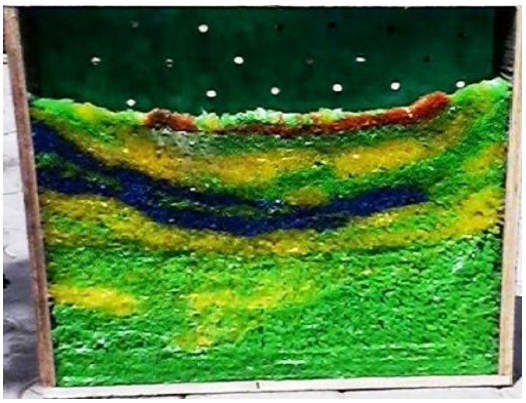

Fig -18: Cross-sectional View of Straws of Honeycomb [14]

After this, the settling chamber screens were fabricated by using three different sieves having specifications as follows

Outermost sieve with M = 1.5 (as shown in Fig. 19)

Mid sieve with M = 9 (as shown in Fig. 20)

Innermost sieve with M = 16 (as shown in Fig. 21)

where M = Holes / inch

Fig -19: Outermost Sieve (M=1.5) [14]

Fig -20: Middle Sieve (M = 9) [14]

Fig -21: Innermost Sieve (M = 16) [14]

After manufacturing the honeycomb, the test section was fabricated using two wooden frames (one at each end) and four transparent Plexiglass panels of thickness 1 mm in between. It is as shown in Fig. 22.

Fig -22: Fabricated Test Section [14]

To accommodate the rod holding the airfoil to be tested aerodynamically, pitot tube and manometer, holes of diameter 10 mm were drilled in the test section.

Finally, a domestic strength fan of 15 inches shroud having two speed levels viz. high and low was attached to the extreme end of the diffuser. The airspeed obtained was between 0 m/s and 20 m/s.

The finally manufactured model of the wind tunnel is as shown in Fig. 23.

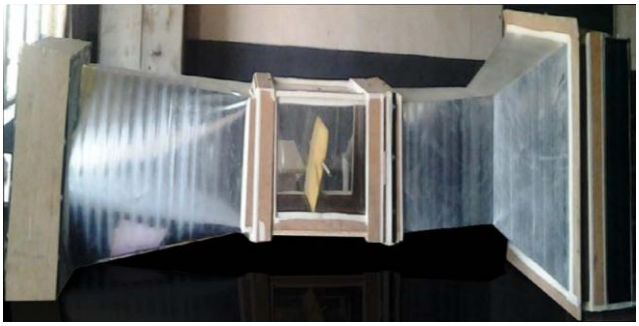

Fig -23: Completely Fabricated Wind Tunnel [14]

The pressure heads (h) and velocities (v) were obtained as shown in Table 1.

Table -1: Readings of Pressure head and Velocity

Sections	Settling Chamber	Test Section	Diffuser
x (mm)	0.8	2	1
h (m) calculated	0.66055	1.650892	0.825
v (m/s) calculated	3.599	5.69122	4.024

The results obtained for lift and drag co-efficient for the test section considering a velocity of 5.7 m/s were as follows: -

Co-efficient of Lift (CL) = 1.30634

Co-efficient of Drag (CD) = 6.14588

The velocity profile obtained is as shown in Fig. 24.

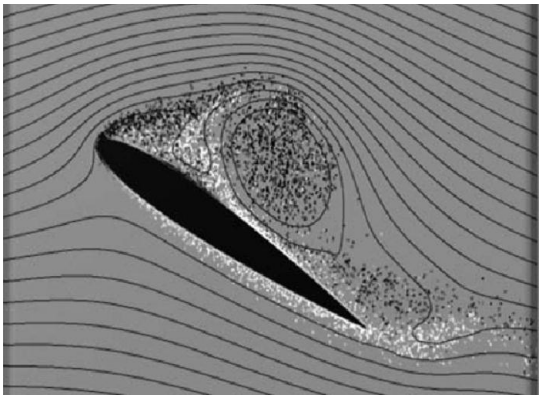

Fig -24: Velocity Profile on the Airfoil [14]

Smoke was used to visualize the air-flow. After testing five different methods of creating smoke viz. strings, incense sticks, mineral oil, smoke-in-a-can and dry ice, the most successful method was the dry ice one. The airfoil which was tested was remotely controlled for understanding what exactly happens on an aircraft when air passes over a wing. The final conclusions drawn were as follows: -

- The velocity profile as shown in Fig. 25 above shows that the smoke flowing inside the test section has high turbulence.
- A velocity of more than 10 m/s is required to show the effect of velocity on the airfoil.
- The wind tunnel is suitable to test airfoils having a weight of less than 0.15 kg.
- Aerodynamics of any high-speed car or airplane can be studied using this wind tunnel using scaled-down models of the same.

[1] discussed the design, construction and various testing processes of a low speed wind tunnel. They broadly discussed wind tunnels and their types along with the construction process that depends on the design parameters. Also, velocity of fluid and drag & lift forces are calculated by conducting experimental analysis of the test specimen.

The main problem this paper tried to address was the construction of a wind tunnel, which otherwise is very expensive to purchase. The focus here was to build a wind tunnel for educational purposes. Some important problem areas identified here were as follows: -

1. Casting and Fabrication –

The casting and fabrication of a wind tunnel is quite expensive. The materials are not easily available.

2. Design Ratio of each Section -

The different designs of wind tunnels are made up of different sizes. Their section sizes and lengths are different. This design variation creates a problem at the time of fabrication.

3. Air will impact the vehicle -

The pressure of air on the vehicle that followed has not been made clear in earlier researches. That means the pressure of air that moved ahead will eventually hamper the speed of the vehicle that followed the first one.

4. Diffuser Set at Different Angles -

If the diffuser is set at different angles and airfoil is set according to basic design, then the effect of profile and drag & lift variation is not clear in earlier researches.

The manufactured wind tunnel with its specifications is as shown in Fig. 25.

- Pitot tube Cv (given) = 0.95
- $\sqrt{2gh}$ = 0.28 (h = 4 mm= .004 m)
- V (velocity middle testing section) = 0.266 m/s
- Fan velocity = 0.353 m/s
- Force of Lift = 3.73 N
- Coefficient of lift = 0.746
- Force of Drag = 0.20 N
- Coefficient of drag = 0.04
- Density of air at 28°C temperature (ρ) = 1.1839 (kg/m^-3)
- Date of reading = 21-11-2014
- Reynolds number = 2.56 x 10^5
- Mach number = 0.008

Fig -25: Manufactured Wind Tunnel with its Specifications [1]

5. Streamlined Body Testing –

Here they have selected an object of length 120mm, made of timber. The diffuser is set at different angles keeping the object constant. The intention of this test was to check whether the velocity increases within the test section if the diffuser angle is changed. Another purpose was to find the variation in the drag and lift forces.

Fig -26: Streamlined Body Testing [1]

Table -2: Manometer Readings for Various Angles of Attack

S. No	Angle of attack	Manometer Readings(mm)				
		P-1	P-2	P-3	N-1	N-2
1	-5°	2	2	3	3	2
2	0°	2	2	2	1	2
3	5°	4	3	2	2	2
4	10°	4	3	3	3	2
5	15°	3	3	3	3	2
6	20°	4	4	3	2	3
7	25°	4	4	4	0	2

The readings were carefully noted down after the testing was done. They noticed that if the diffuser setting was changed upwards and downwards, then in upward position the pressure increased, and the negative point is decreased. While, if the diffuser is set in downward position then the pressure is decreased, and the negative point is increased. The performance of the airfoil was better at 15˚ angle of attack.

Table -3: Drag and Lift Force Readings at Different Points [1]

S. No.	Angle of attack	Drag force (N)	CD	Lift force (N)	CL
1	-5°	0.23	0.046	3.953	0.791
2	0°	0.20	0.04	3.727	0.746
3	5°	0.20	0.04	3.727	0.746
4	10°	0.149	0.030	7.122	1.424
5	15°	0.412	0.08	4.368	0.874
6	20°	0.294	0.059	3.139	0.629
7	25°	0.735	0.147	4.71	0.942

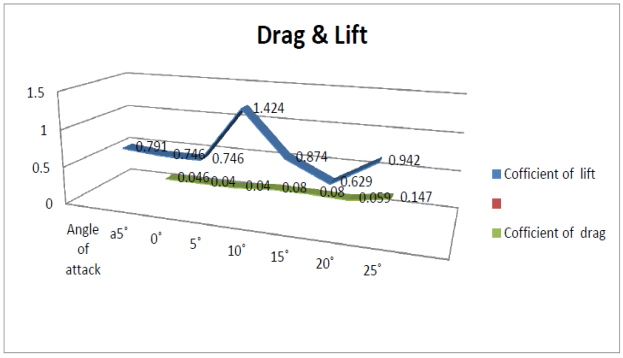

Fig -27: Graph of Drag and Lift Co-efficients [1]

They also noticed that the velocity increases when the diffuser is set at different angles.

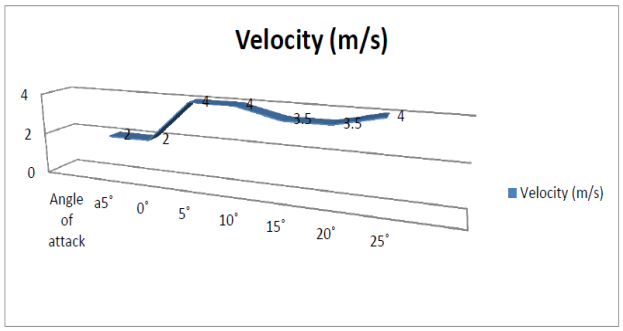

Fig -28: Graph of velocity profile [1]

Table -4: Readings for Diffuser Set at Different Angles [1]

S. No.	Angle of attack	Pitot tube and manometer reading (mm)	V (m/s)
1	-5°	2	0.188
2	0°	2	0.188
3	5°	4	0.266
4	10°	4	0.266
5	15°	3.5	0.249
6	20°	3.5	0.249
7	25°	4	0.266

6. Object is Rotated at Different Angles, but System is Set to Basic Design –

The purpose of this test was to see the changes in drag and lift forces when the object is rotated at different angles while the diffuser is set to its basic design. Both, upward and downward readings are found out in this test. In upward test, the air foil performs better at 15° angle of attack. And in downward test, the air foil performs better at 15° & 20° angle of attack.

Table -5: Object Moved by Different Angles [1]

S.No.	Angle of attack	Manometer Readings (mm)					Position of object
		P-1	P-2	P-3	N-1	N-2	
1	25°	3	3	2	5	3	
2	20°	3	4	4	5	3	
3	15°	4	3	3	4	2	
4	10°	4	4	3	4	2	
5	5°	4	3	2	3	2	
6	0°	4	3	2	2	2	
7	5°	5	4	3	3	2	
8	10°	3	4	3	3	2	
9	15°	3	3	2	2	2	
10	20°	4	3	3	3	1	
11	25°	3	3	3	3	2	

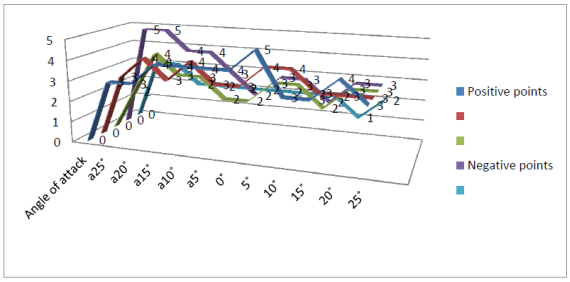

Fig -29: Graph of Positive and Negative Pressure due to the Moved Object [1]

Table -6: Drag and lift forces [1]

S. No.	Angle of attack	Drag force	CD	Liftforce	CL	Position of object
1	25°	1.75	0.23	2.41	0.483	
2	20°	1.66	0.332	2.326	0.465	
3	15°	1.571	0.314	2.103	0.421	
4	10°	1.275	0.255	1.354	0.271	
5	5°	0.37	0.074	1.02	0.204	
6	0°	0.20	0.04	3.7278	0.745	
7	5°	1.589	0.318	6.072	1.22	
8	10°	2.736	0.547	7.740	1.548	
9	15°	4.267	0.853	6.562	1.312	
10	20°	5.98	1.196	8.535	1.707	
11	25°	7.69	1.538	8.93	1.786	

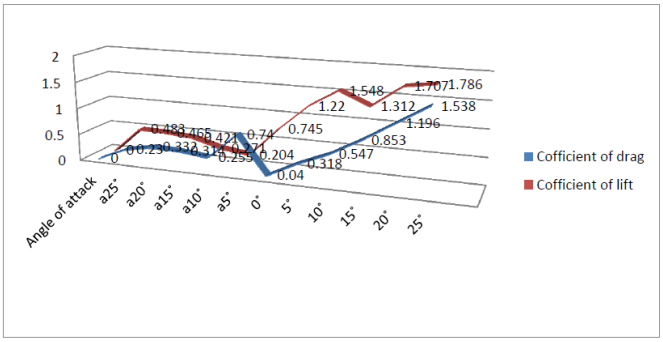

Fig -30: Graph of Drag and Lift Co-efficients [1]

7. Result of Last Experiment -

When the vehicle is in running condition, then the pressure of air that moved ahead will eventually hamper the speed of the vehicle that followed the first one. The hampering by pressure is little if the vehicle is streamlined. The hampering is high if the vehicle is a half sphere.

Fig -31: Half-shaper Medium in Front of Airfoil (horizontal) [1]

Table -7: Readings for Half-shaper Medium in Front of Airfoil (horizontal) [1]

S. No.	Angle of attack	Manometer readings (mm)				
		P-1	P-2	P-3	N-1	N-2
1	0°	1.5	3	3	2	2.5

Table -8: Readings for Half-shaper Medium in Front of Airfoil (vertical) [1]

S. No.	Angle of attack	Manometer readings (mm)				
		P-1	P-2	P-3	N-1	N-2
1	0°	2	2.5	2.5	1.5	2

Finally, they tested for effect of pressure/velocity on different angles of tyre. The scaling for tyres was as follows: -

1 mm = 10 mm

Fig -32: Testing Pressure Point of Tyre [1]

Table -9: Readings for Pressure Point of Tyre

S. No.	Angle of attack	Manometer readings (mm)		
		P-1	P-2	P-3
1	0°	5	4	2

The result was that, when the tyre was in moving condition, then the pressure is different for each angle of attack. They marked three points at each at 0˚, 90˚ and 180˚respectively. In each point pressure was different. It was seen that there was no negative pressure in the tyre.

[10] designed and manufactured the following components of their wind tunnel: -

1. Settling Chamber and Honeycomb Structure -

Two honeycomb sections were fabricated by the researchers. Four pieces of plywood of 1000 mm long and 19.05 mm thick each were cut. They were assembled together by fevicol and nails to form a cube. The honeycomb section was made of circular pipes of aluminium with 100 mm length and inner and outer diameters of 31 mm and 32 mm respectively. The tubes were stuck together by an adhesive glue. The dimensions of the settling chamber are shown in Fig. 33.

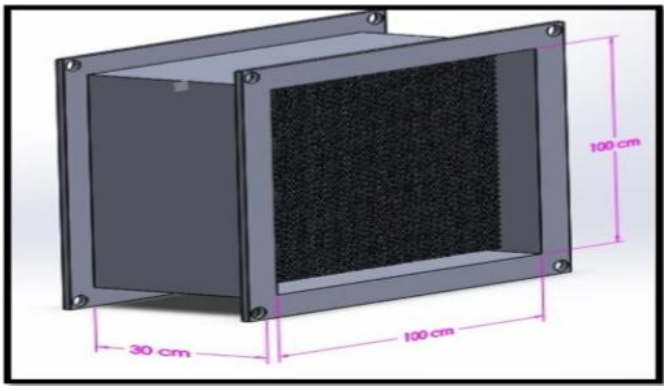

Fig -33: CAD model of settling chamber [10]

2. Contraction Cone -

They designed the contraction cone after the settling chamber. The contraction cone was manufactured with the help of plywood, nail, fevicol. A honeycomb section was also added at the end of the contraction section near the test section to produce more uniform air in the test section. A damper was also added at each joint. The fabricated damper along with the CAD model and manufactured contraction cone is as shown in Fig. 34 and Fig. 35 respectively.

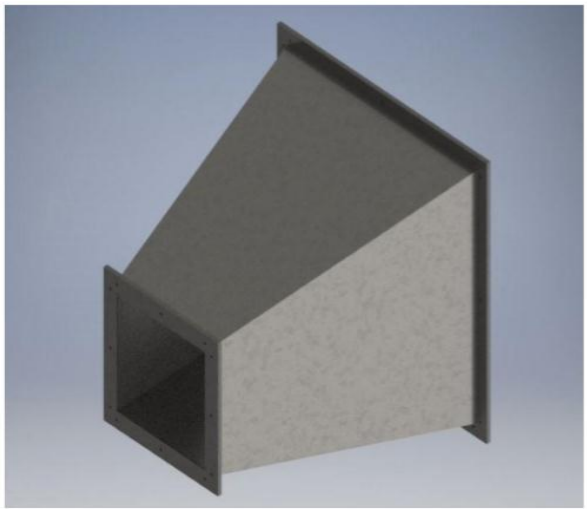

Fig -34: CAD Model of Contraction cone [10]

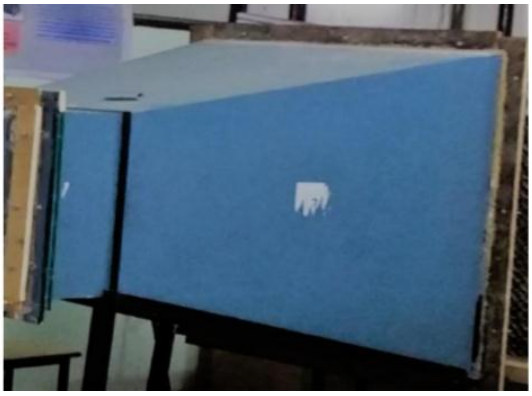

Fig -35: Manufactured contraction cone [10]

Table -10: Specifications of Contraction Cone

Parameters	Dimensions
Inlet cross section area	1000mm×1000 mm
Outlet cross section area	500mm×500mm
Length	1180mm
Contraction ratio	4:1
Contraction angle	24^0

3. Test Section -

They designed the test section after the contraction cone. The test section was made up of plywood and fibre glass. Its top and bottom sections were made up of plywood and the side sections were made up of fibre glass. All the sides were assembled to form a cuboid shape. The wind speed that was achieved in the test section was 20 m/s, along with that uniform air outlet was also achieved. Dampers were added. The CAD model and manufactured test section are as shown in Fig. 36 and Fig. 37.

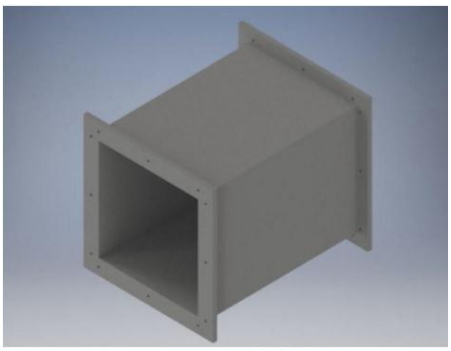

Fig -36: CAD model of Test Section [10]

Fig -37: Manufactured Test Section [10]

4. Diffuser -

The diffuser, whose CAD model is as shown in Fig. 38 was fabricated using plywood, fevicol, and nails. Prior to that, it was designed according to the dimensions as shown in Table 11.

Table -11: Specifications of Diffuser

Inlet cross section of diffuser	500mm×500mm
Outlet cross section of diffuser	700mm×700mm
Length of diffuser	1600mm
Angle of inclination	7^0

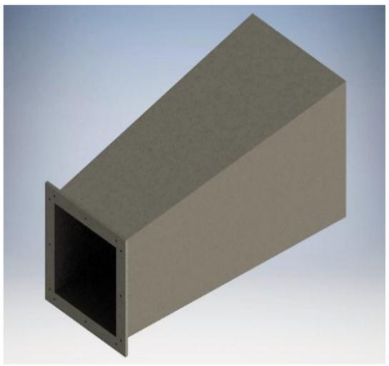

Fig -38: CAD model of diffuser [10]

5. Drive Unit and its Foundation -

The specifications of the drive unit are as shown in Table 12.

Table -12: Specifications of Drive Unit

Component	Specification
Motor power	7.5 HP
Maximum Speed of motor	1440 rpm
Types of motor	3 phase induction motor
Types of fan	Axial fan
Fan diameter	1000

Fig -39: Fan and its Housing [10]

6. Assembly of Wind Tunnel -

Firstly, the foundation for the drive unit was made and the fan was mounted on it. The settling chamber was connected to the driven unit with damper in between them. The dimensions of the foundations were 1160 mm X 1160 mm cross-section with a hole whose diameter was 980 mm was used to connect the fan and the settling chamber. The honeycomb section was mounted in the settling chamber. The contraction cone was connected to the settling chamber with nuts and bolts with a damper between them. After that the test section and the diffuser were assembled to the setup. After the assembly is done the fan was started and all the joints were checked for leakage and the line of alignment was also checked. The CAD model for the assembled wind tunnel is as shown in Fig. 40.

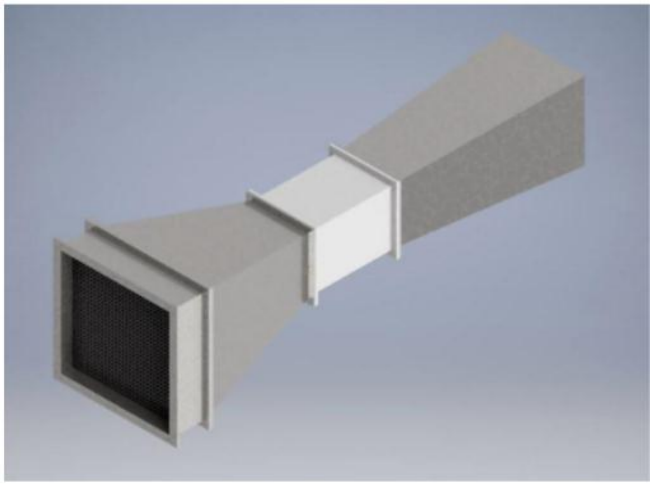

Fig -40: CAD Assembly of Wind Tunnel [10]

7. Testing Procedure -

Semi-airfoil section was manufactured to test the variation of velocity and pressure in the wind tunnel. Velocity changes in the tunnel were measured using a digital anemometer and a digital pitot tube was used to measure the pressure differences. In the first step the required units for velocity (m/s) and for pressure (mbar) were set up. The tunnel was tested without any test object first to check the uniformity of wind flow in the wind tunnel. Then the test chamber was divided into number of points and they were marked as shown in Fig. 41.

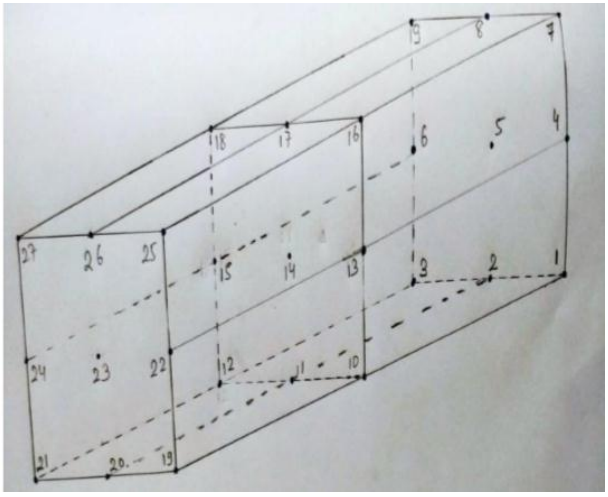

Fig -41: Velocity and Pressure Measurement Points [10]

The wind tunnel was tested at three different points of the test section. The three sections shown in the above diagram are the inlet (1-9), the middle part (10-18) and the end part (19-27).

When the wind tunnel was tested a leakage was found in the upper section of the test section. Due to the leakage, both velocity and pressure were affected. It was observed that velocity decreased and the pressure increased from the bottom side to upper side of the wind tunnel. From the left to right side there were no changes in the velocity but at the middle portion there was increase in velocity due to the leakage. From the data measured it was assumed that the maximum velocity of the wind was at the bottom portion of the test section. The uniform velocity which was obtained in the test section was 20 m/s and the uniform air pressure was 36 bar.

8. Test Result with Solid Object inside the Test Section -

Before the semi-airfoil was tested in the test section, markings were made on the test objects. The object was tested at these marked points. The shape of the object was like the equation of curve given by Y = X2 along the length, with its origin in the middle portion at maximum height. The object had constant shape along the width. The dimensions of the object as shown in Fig. 42 were as follows: -

Length of the object = 39 cm

Width of the object = 26.5 cm

Maximum height at middle portion of length = 15 cm

Fig -42: Model of Semi-airfoil for Testing [10]

The object was divided into number of small elements with the length of each element at top section being 5 cm and width of the object being 8.9 cm. Each node on the object was marked with a specific number. There were 44 nodes marked on the test object. The velocity and pressure were measured at these 44 node points. The pressure in between two nodes was calculated by using interpolation. The test object was tested under varying conditions and its effect on the test object were measured. According to the data collected, pressure versus velocity graphs along the length of the test section were plotted for three cases as shown in Fig. 43 to Fig. 50.

Case I: Graph along the marks (1-5-9-13-17-21-25-29-33-27-41) on the object:

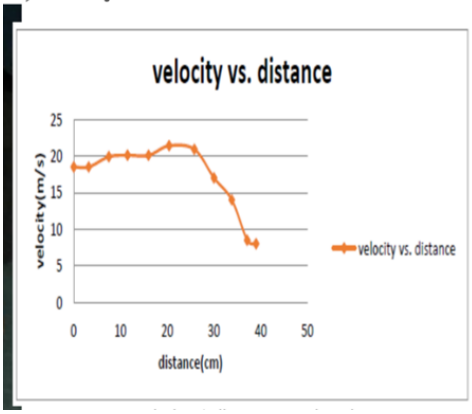

Fig -43: Velocity vs Distance Curve (Case I) [10]

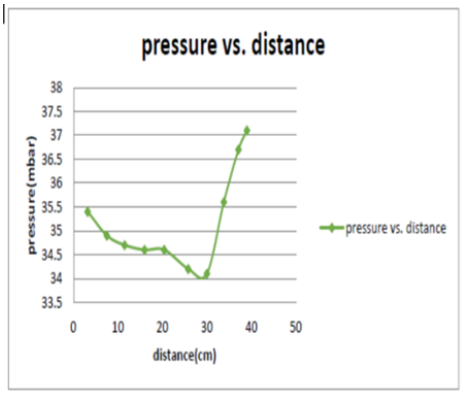

Fig -44: Pressure vs Distance Curve (Case I) [10]

Case II: Graph along the mark (2-6-10-14-18-22-26-30-34-38-42) on the object:

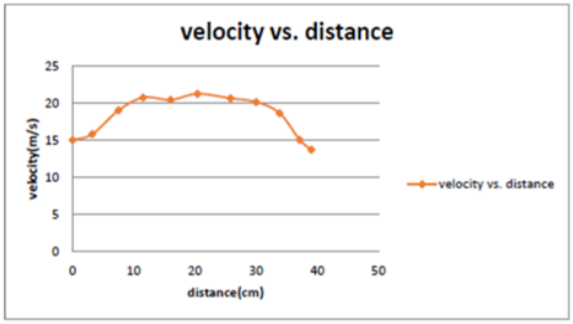

Fig -45: Velocity vs Distance Curve (Case II) [10]

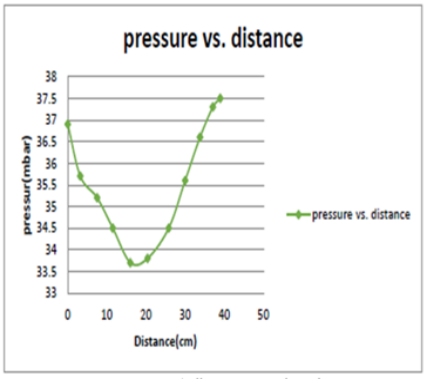

Fig -46: Pressure vs Distance Curve (Case II) [10]

Case III: Graph along the curve (3-7-11-15-19-23-27-31-35-39-43) on the testing object

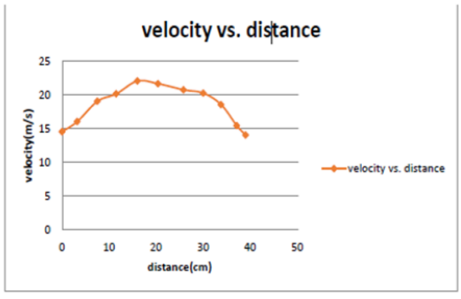

Fig -47: Velocity vs Distance Curve (Case III-1) [10]

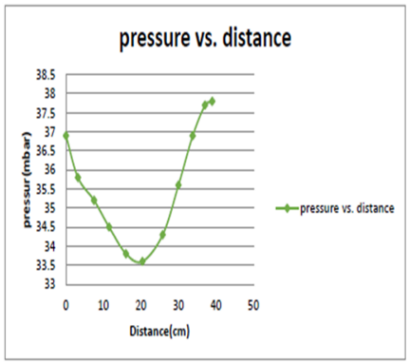

Fig -48: Pressure Vs Distance Curve (Case III-1) [10]

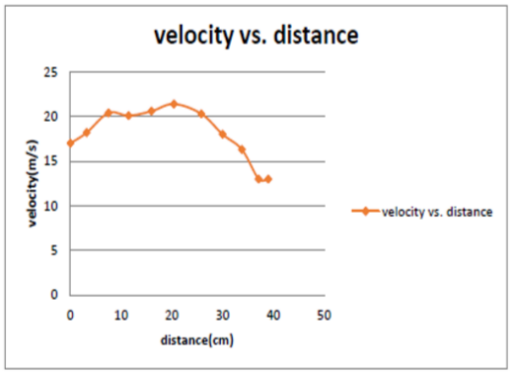

Fig -49: Velocity Vs Distance Curve (Case III-2) [10]

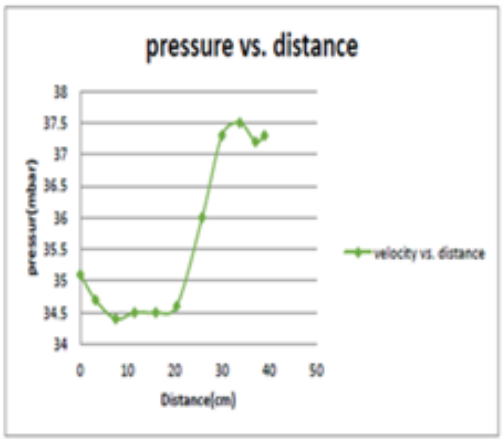

Fig -50: Pressure Vs Distance Curve (Case III-2) [10]

[12] divided the design based on the wind tunnel components as follows: -

1. Test Section -

The first step of the wind tunnel design was defining the dimensions of the test section, its shape and the desired air velocity. A test section of square cross-section of 0.9 m side with an air velocity of 40 m/s was selected. The test chamber has to be in the range of 0.5 - 3 times the hydraulic diameter. The length of the test section was set to 1.3 times the hydraulic diameter of the test section. According to this parameter the length of the test section was 1.35 m. The CAD design of the test section is shown in the Fig. 51.

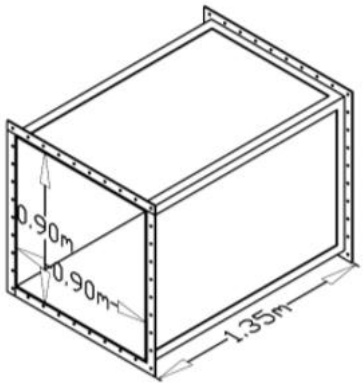

Fig -51: CAD Design of Test Section [12]

2. Contraction Cone -

The area ratio (AR) of 8 was chosen for the contraction cone. Normally, a contraction ratio between 6 - 10 is selected. The length of the contraction section was found to be 0.38 m considering these parameters. The CAD model of the contraction cone is as shown in Fig. 52.

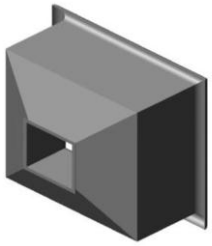

Fig -52: CAD Design of Contraction Cone [12]

3. Diffuser -

For the diffuser design area ratio of less than 2.5 was selected and the diffuser angle of 50 to 70 was selected. According to these considerations, the outlet diameter of 122 cm was selected. The minimum length of the diffuser was found out from the equation given below -

$$\vartheta_e = arc\ tan\left(\frac{1}{2}\frac{\sqrt{A_R}-1}{L/D_{h1}}\right) \quad \text{..... (1)}$$

where - Dh1 is the inlet section's hydraulic diameter which is equal to half of included angle of diffuser cone

The minimum length of the diffuser was found out to be 2.34 m. The length satisfying the above criteria was 3.7 m. The CAD design of the diffuser section is as shown in Fig. 53.

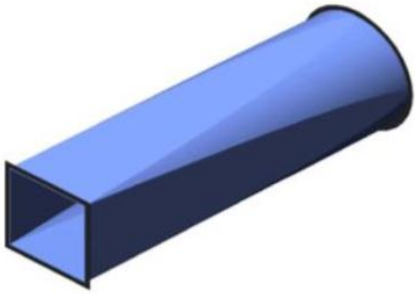

Fig -53: CAD Design of Diffuser Section [12]

4. Settling Chamber -

A settling chamber of length 0.5 times the inlet diameter is usually used. According to this condition the length of the settling chamber was 1.105 m.

5. Honeycomb -

According to the researchers, the key factors affecting the honeycomb design are length (Lh), cell diameter (Dh) and the porosity (βh). The honeycomb porosity was defined as the ratio of actual flow cross-section area over the total cross-section area. The formula was given as-

$$\beta_h = \frac{A_{flow}}{A_{total}} \quad \text{..... (2)}$$

The two criteria were verified by,

$$6 \leq \frac{L_h}{D_h} \leq 8 \quad \text{..... (3)}$$

And the second was verified by,

$$\beta_h \geq 0.8 \quad \text{..... (4)}$$

The parameters of the honeycomb section are given in Table 13.

Table -13: Parameters of Honeycomb

Parameters	Symbols	Value	Units
Cell hydraulic diameter	D_h	2.12	cm
Length of honeycomb	L_h	12	cm
Number of cells	N	38000	
Length to diameter ratio	L_h/D_h	6	
Honeycomb porosity	β_h	0.8	

6. Screens -

As per the researchers, the screens are an important part of the wind tunnel as they reduce turbulence. To be effective in reducing turbulence the porosity of the screen should be in the range 0.58 to 0.8. The screens having porosity more than 0.8 are ineffective in reducing turbulence and screens having porosity less than 0.58 create flow instability. The area occupied by the screen was calculated by using the following equation

$$n_w l d_w + n_w l d_w - n_w (n_w d_w^2) \quad \text{..... (5)}$$

Where, dw is the wire diameter, nw is the generic wire number in the mesh and l is the cross-section of the settling chamber. The last term in the above formula takes into account the area where the wires of the screen cross each other shown in Fig. 54.

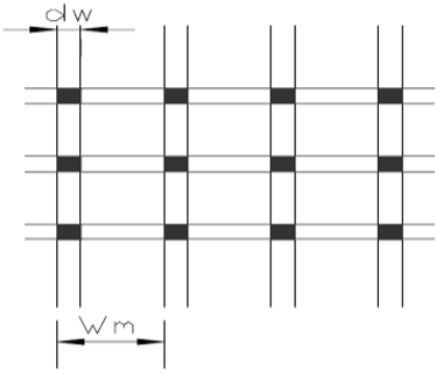

Fig -54: Single Mesh Sample [12]

The porosity of the honeycomb section was calculated using the following equation

$$\beta_s = \frac{A_{flow}}{A_{total}} = \frac{l^2 - 2n_w l d_w + n_w^2 d_w^2}{l^2} = 1 - 2n_w \frac{d_w}{l} + \frac{n_w^2 d_w^2}{l^2} \quad \text{.... (6)}$$

By simplifying the above equation,

$$\beta_s = \left(1 - \frac{n_w d_w}{l}\right)^2 \quad \text{..... (7)}$$

The screen mesh density was calculated by using the formula,

$$\rho_m = \frac{n_w}{l} \quad \text{..... (8)}$$

The inverse of the mesh density gives the formula for screen mesh density given by,

$$w_m = \frac{1}{\rho_m} \quad \text{..... (9)}$$

By taking the screen mesh density into account, the equation of porosity became

$$\beta_s = (1 - d_w \rho_m)^2 \quad \text{..... (10)}$$

Table 14 shows the screen characteristics used in the wind tunnel

Table -14: Characteristics of Screens

Description	Symbol	Unit	M_1	M_2
Mesh wire diameter	d_w	mm	0.58	0.45
Mesh divisions	w_m	mm	2.50	1.95
Screen porosity	β_s	-	0.59	0.59

7. Pressure Losses -

According to the researchers, the pressure losses in the wind tunnel occur as consecutive losses that take place in different sections. The overall pressure loss (Δpglobal) is equal to the pressure gained by the fan. Considering a wind tunnel component i, the pressure loss (Δpi) in that section can be written as a product of a constant Ki and the dynamic pressure at the entrance of the component. The formula for calculating the constant is given by the equation,

$$K_i = \frac{\Delta p_i}{\frac{1}{2}\rho_i c_i^2} \quad \text{..... (11)}$$

Where, ci is the mean flow velocity in the ith component.

Using the above formula, the loss coefficients for each component were calculated. Table 15 shows the pressure drop for each component of the wind tunnel. The addition of all the pressure drops gave the total pressure drop across the wind tunnel

Table -15: Values of Pressure Drop

Components	Pressure loss, Δp [Pa]
Test section	9.76
Diffuser	61.42
Honeycomb	3.1
Screen 1	7.65
Screen 2	9.46
Contraction cone	2.05
Total Pressure loss	93.44

By assuming null relative pressure value in the test section and depending on the value of coefficients and pressure drop values, the relative pressure values in the wind tunnel were calculated. The ideal value without energy loss can be found out by the equation given below,

$$P_{out} - P_{in} = \frac{1}{2}\rho(u_{in}^2 - u_{out}^2) \quad \text{..... (12)}$$

And the real value with energy losses can be found out by the equation,

$$P_{out} - P_{in} = \frac{1}{2}\rho(u_{in}^2 - u_{out}^2) - \Delta P_{loss-in-out} \quad \text{..... (13)}$$

where, ΔPloss-in– out is the value of pressure loss between inlet and the outlet of the cross-section that are denoted by the Ki factor.

The variation in the static pressure in the wind tunnel is shown in Fig. 55.

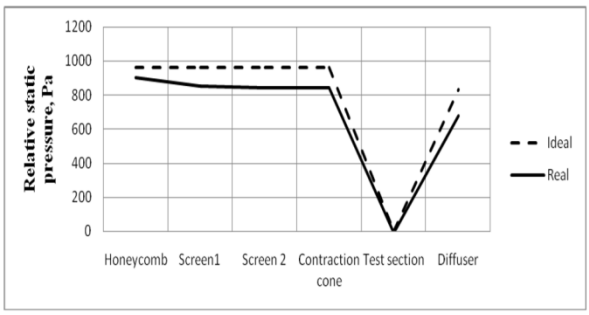

Fig -55: Relative Static Pressure in the Wind Tunnel [12]

From the figure, the comparison between real and ideal pressure values can be seen. It was observed that the real values are always smaller than ideal values due to the pressure losses in the wind tunnel.

Fig. 56 shows the incremental pressure losses that occur in the tunnel.

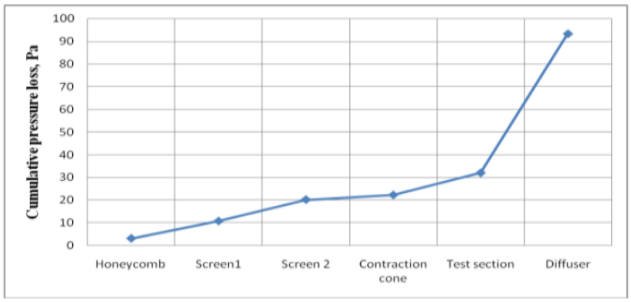

Fig -56: Cumulative Pressure Losses in Wind Tunnel [12]

Fig. 57 shows the pressure losses in each section of the wind tunnel. It was observed that maximum pressure losses took place in the diffuser section and the minimum in the contraction section.

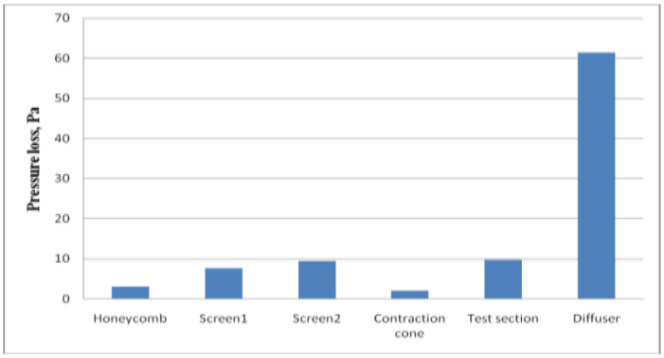

Fig -57: Pressure Losses in Each Section [12]

The manufacturing and assembly details are as follows: -

1. Test Section -

The test section was constructed according to the design. It could be seen from three sides i.e. front, back and top. To make the object inside the test section visible, acrylic sheet was used which was bolted to the test section frame. An opening was also provided to keep the models inside the test section easily. The leakages were sealed using M-seal.

2. Contraction Cone, Settling Chamber & Diffuser -

These were constructed using 3 mm thick mild steel plates in order to reduce the construction costs. An important thing is to correctly fabricate the diffuser section as its one end is rectangular and another end is circular in cross-section.

3. Honeycomb and Screens -

To reduce the air turbulence and increase the flow uniformity, two screens were used. Readymade screens were purchased from the market while honeycomb was constructed in the lab manually. Fig. 58 shows the constructed honeycomb.

Fig -58: Constructed Honeycomb [6]

4. Assembly of the Wind Tunnel -

The wind tunnel was assembled and installed in a mechanical engineering workshop. It is as shown in Fig. 59.

Fig -59: Assembled Wind Tunnel [12]

Results and Discussion -

After the installation of the wind tunnel, different data was taken down to construct the velocity profile in the test section whereas pressure readings were recorded at different points. All data was taken at maximum air velocity. Fig. 60 shows the horizontal velocity profile at different points in the test section from the front wall.

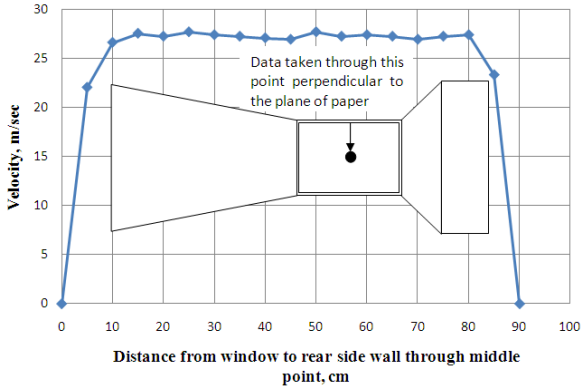

Fig -60: Horizontal velocity profile [12]

From the horizontal velocity profile, it was seen that 10 cm from the rear front wall, the velocity of flow was almost linear up to 80 cm. Velocity near the wall was of gradually increasing nature and this was because of the boundary layer. So, the maximum boundary layer thickness was found to be 10 cm and the effective air flow velocity was found at a length of 70 cm which was located 10 cm from both the walls. In percentage, the effective flow length was about 76% and boundary layer region in each wall was about 12% of the total width of the tunnel. The mean free stream velocity was found out to be about 28 m/s. Fig. 61, Fig. 62 and Fig. 63 show the vertical velocity profile at different distances from the bottom to top wall of the test section while the pressure difference reading was taken at a distance of 5 cm, 60 cm and 115 cm respectively from the test section inlet.

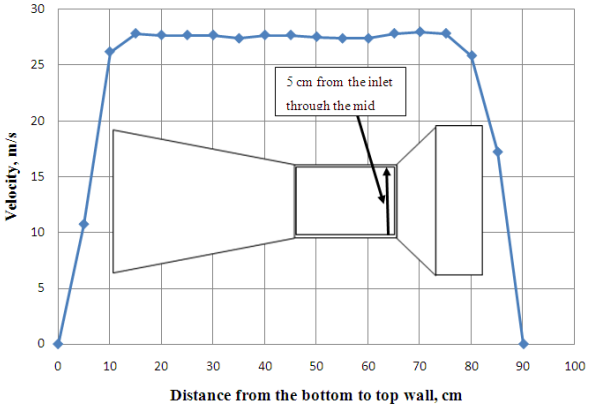

Fig -61: Vertical velocity profile at a distance 5 cm [12]

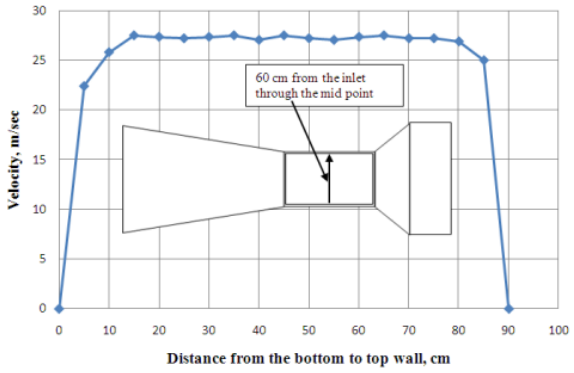

Fig -62: Vertical velocity profiles at a distance 60 cm [12]

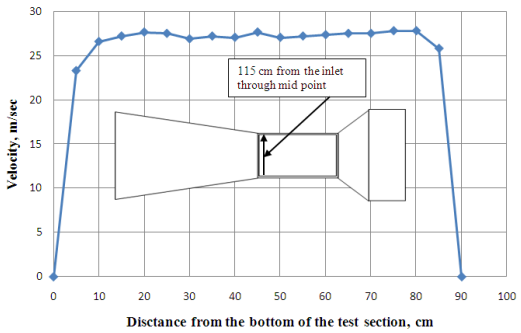

Fig -63: Vertical velocity profiles at a distance 115 cm [12]

Fig. 64 shows the combined vertical velocity profile.

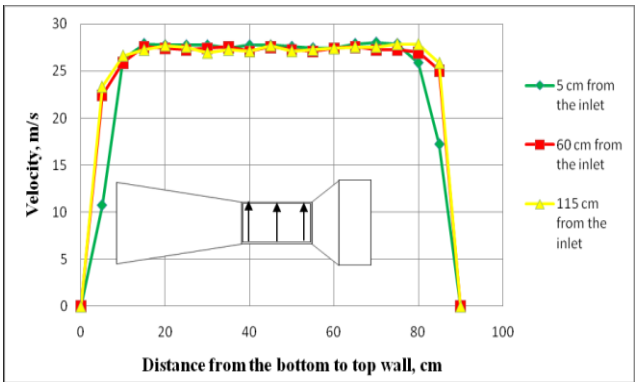

Fig -64: Vertical velocity profiles at three position [12]

From the velocity profiles, it was clear that the mean velocity in the test section was almost linear. At 5 cm from the test section inlet, air velocity close to the wall was much less than the other positions (at 60cm and 115 cm). The maximum velocity was also found at 5 cm position. This happened because of the effect of the contraction outlet due to which vena-contracta is formed. In case of 60 cm and 115 cm positions, velocity profile is almost similar which indicates that mean flow velocity throughout the test section was identical. For all cases, velocity was gradually increasing near the wall because of the boundary layer formed. This boundary layer region was approximately 12% of the total height of the test section in each side. So, the effective flow height was found to be approximately 76% of the total height of the test section. The effective flow region was 10 cm from the bottom wall to 10 cm below the top wall. In case of vertical measurements, the mean flow velocity in the effective flow region was about 28 m/s.

5. CONCLUSIONS

According to the researchers, the purpose of their research work was to design, construct and conduct performance tests of a short length subsonic wind tunnel to verify its adequacy for aerodynamic analysis applications as well as to simulate the velocity profile at different position of the test section. The wind tunnel was designed considering a mean test section speed 40 m/s and all factors were considered to make it as short as possible. Then, it was fabricated as accurately as possible. The length of the constructed wind tunnel was about 7.35 m and a free stream velocity was found approximately 30 m/s. A comparison between the newly constructed wind tunnel and the wind tunnel built at NASA and MIT (USA) of approximately same test section is shown in Table 16. From the comparison it was clear that the overall length of newly designed wind tunnel was much shorter than the other two. Besides this, the construction cost of the wind tunnel was about $8500 which was much less than the one available in the market of the same size.

Table -16: Comparison of Existing Wind Tunnels

Parameters	New Tunnel	NASA(Small) Tunnel	MIT (USA) Tunnel
Test section	0.9 m × 0.9 cm	0.9 m × 0.9 m	0.85 m × 0.85 m
Mean velocity	28 m/s	25 m/s	40 m/s
Test section length	1.35 m	3 m	2.8 m
Overall length	7.35 m	13 m	11 m

The detailed specifications of the wind tunnel built are shown in Table 17.

Table -17: Specifications of Built Wind Tunnel

Parameters	Value
Type	Open circuit
Test section length	1.35 m
Test section cross section	0.90 m × 0.90 m
Mean air velocity range	28 m/s
Overall length	7.35 m
Effective region in the test section	76% of width or height
Boundary layer region	12% of width or height from every wall
Contraction ratio	8
Honeycomb cell diameter, length	0.02 m, 0.125 m
Number of screens	2
Settling chamber cross section	2.55 m × 2.55 m
Motor and Fan	3-phase 20 kW, 10 blades

The researchers concluded that the newly designed tunnel was therefore a very good device to provide parallel steady flow with uniform speed through the test section without excessive turbulence and can be used effectively in different aerodynamic researches. [12]

An important point of conclusion was that the air foil performs better at 15˚ angle of attack. They concluded that if streamlined design rules are followed then each vehicle performs better. This will also improve the velocity of vehicle. Another important part of a vehicle are the tyres. Testes were done on them which showed no negative pressure in the tyre. They reached a drag coefficient of 0.04. This is a good sign for future research. Most importantly, the cost of the constructed wind tunnel was less than that available in the market [1].

Wind tunnel screens are normally made up of metal wires which are inter-woven to make square or rectangular meshes. Nowadays, nylon or polyester is also being used. The variations in longitudinal mean velocity can be minimized to almost zero by using a screen having a pressure drop co-efficient of about 2. [2]

The shape, size, material selection and manufacturing process is an important part of wind tunnel manufacturing. Velocity increases when the height of the object gradually increases and the pressure is decreased along the length of the object. The pressure energy was converted into kinetic energy when the height of the object increased and as the height of the object decreased this kinetic energy was again converted back to pressure energy. The lift and drag forces depend on the shape and size of the object. [10]

In this paper a small size wind tunnel is designed and it is tested by using state-of-art CFD simulation. The CFD simulations validated the design as a uniform dynamic pressure along with uniform fluid velocity was obtained across the test section. Acceptable flow quality was shown as there was minor cross flow and up flow angles. The cost of the wind tunnel was well below the wind tunnels available in the market. The performance of wind tunnel was adequate when it was tested for various simulations. [8]

A 10 feet length subsonic wind tunnel was designed and manufactured. The effect of the wind on the NACA 63-215 airfoil was tested in the wind tunnel. Airfoil of weight less than 0.15 kg can be tested in this wind tunnel. [14]

ACKNOWLEDGEMENT

We would like to express our sincere thanks and gratitude to all the authors and researchers for their work on design, manufacturing and testing of low speed open-circuit wind tunnels.

REFERENCES

[1] Bapu Joglekar, Rana Manoj Mourya, "Design, Construction and Testing Open Circuit Low Speed Wind Tunnel", International Journal of Electrical and Electronics Research Vol. 2, Issue 4, pp: (271-285), Month: October - December 2014.

[2] R. D. Mehta and P. Bradshaw, "Design rules for small low speed wind tunnels", Aeronautical Journal November 1979, 443–449.

[3] Miguel A. González Hernández,Ana I. Moreno López, Artur A. Jarzabek, José M. Perales Perales, Yuliang Wu and Sun Xiaoxiao, "Design Methodology for a Quick and Low-Cost Wind Tunnel", InTech Open Science.

[4] Barlow, Jewel B. Rae Jr, William H. Pope Alan. "Low Speed Wind Tunnel Design", 3rdEdition, John Wiley and Sons Inc. New York, NY, 1999.

[5] Rodney J. Kubesh and Bret W. Allie, "A wind tunnel for an undergraduate laboratory", International Journal of Mechanical Engineering Education.

[6] B.Navin Kumar, K.M.Paramasivam, M.Prasanna A.Z.G Mohamet Karis, "Computational fluid dynamics analysis of aerodynamic characteristics of NACA 4412 VS S809 airfoil for wind turbine applications", International Journal of Advanced Engineering Technology, Vol. VII/Issue III/July-Sept.,2016/168-173.

[7] Louis Cattafesta, Chris Bahr, and Jose Mathew, "Fundamentals of Wind-Tunnel Design", Encyclopedia of Aerospace Engineering.

[8] Peter John Arslanian, Dr. Payam Matin, "Undergraduate research on conceptual design of a wind tunnel for instructional purposes", American Society for Engineering Education, 2012.

[9] Vikas Dalal, "Designing and Construction of Low Speed Wind Tunnel WiWu To Investigate the Robustness of Small Model Aircrafts and Launcher Controllers", Luleå University of Technology Department of Computer Science, Electrical and Space Engineering.

[10] Nagendra Kumar Maurya, Manish Maurya, Avdhesh Tyagi, Shashi Prakash Dwivedi, "Design & Fabrication of Low Speed Wind Tunnel and Flow Analysis", International Journal of Engineering & Technology, 7 (4.39) (2018) 381-387.

[11] Mike Fitzgerald, "Build a Wind Tunnel", Tech directions, Prakken Publications, Inc; 2005.

[12] Md. Arifuzzaman, Mohammad Mashud, "Design Construction and Performance Test of a Low-Cost Subsonic Wind Tunnel", IOSR Journal of Engineering (IOSRJEN), Volume 2, Issue 10 (October 2012), PP 83-92.

[13] Mauro S, Brusca S., Lanzafame R., Famoso F., Galvagno A. and Messina M., "Small-Scale Open-Circuit Wind Tunnel: Design Criteria, Construction and Calibration", International Journal of Applied Engineering Research

ISSN 0973-4562 Volume 12, Number 23 (2017) pp. 13649-13662.

[14] Mansi Singh, Neha Singh & Sunil Kumar Yadav, "Review of Design and Construction of an Open Circuit Low Speed Wind Tunnel", Global Journal of Researches in Engineering Mechanical and Mechanics Engineering Volume 13 Issue 5 Version 1.0 Year 2013.

BIOGRAPHIES

Shreyas S. Kharolkar –
He is pursuing B.E. in Mechanical Engineering at MIT, Pune.

Sarvesh S. Kale –
He is pursuing B.E. in Mechanical Engineering at MIT, Pune.

Prof. Ketan V. Karandikar –
Presently working as a Lecturer in Mechanical Engineering Department of MAEER's MIT Polytechnic, Pune, Maharashtra, India. He has a teaching experience of 7 years. He has published more than 5 research papers in international journals and conferences. Recently he has won the Best Research Paper Award at 2nd World Congress on Engineering & Applications organized by ASRES, held at Pattaya, Thailand.

Prof. Pushkaraj D. Sonawane –
Currently Assistant Professor at the School of Mechanical Engineering, MIT World Peace University, Pune (INDIA). His research interests are focused on "Materials Processing", "Concentrated Solar Energy", "Materials Engineering" and "Mechanical Engineering Design". He has published more than 25 research papers in various international journals.